Substitution of the Sixth Axial Ligand of *Rhodobacter capsulatus* Cytochrome c_1 Heme Yields Novel Cytochrome c_1 Variants with Unusual Properties†

Elisabeth Darrouzet,‡ Sevnur Mandaci,§ Jun Li,|| Hong Qin,|| David B. Knaff,|| and Fevzi Daldal*,‡,§

Department of Biology, Plant Science Institute, University of Pennsylvania, Philadelphia, Pennsylvania 19104, RIGEB, Marmara Research Center, TUBITAK, Gebze 41470, Turkey, and Department of Chemistry and Biochemistry, Texas Tech University, Lubbock, Texas 79409

Received January 27, 1999; Revised Manuscript Received May 3, 1999

ABSTRACT: The cytochrome (cyt) c_1 heme of the ubihydroquinone:cytochrome *c* oxidoreductase (bc_1 complex) is covalently attached to two cysteine residues of the cyt c_1 polypeptide chain via two thioether bonds, and the fifth and sixth axial ligands of its iron atom are histidine (H) and methionine (M), respectively. The latter residue is M183 in *Rhodobacter capsulatus* cyt c_1, and previous mutagenesis studies revealed its critical role for the physicochemical properties of cyt c_1 [Gray, K. A., Davidson, E., and Daldal, F. (1992) *Biochemistry 31*, 11864−11873]. In the homologous chloroplast b_6f complex, the sixth axial ligand is provided by the amino group of the amino terminal tyrosine residue. To further pursue our investigation on the role played by the sixth axial ligand in heme−protein interactions, novel cyt c_1 variants with histidine−lysine (K) and histidine−histidine axial coordination were sought. Using a *R. capsulatus* genetic system, the cyt c_1 mutants M183K and M183H were constructed by site-directed mutagenesis, and chromatophore membranes as well as purified bc_1 complexes obtained from these mutants were characterized in detail. The studies revealed that these mutants incorporated the heme group into the mature cyt c_1 polypeptides, but yielded nonfunctional bc_1 complexes with unusual spectroscopic and thermodynamic properties, including shifted optical absorption maxima (λ_{max}) and decreased redox midpoint potential values (E_{m7}). The availability and future detailed studies of these stable cyt c_1 mutants should contribute to our understanding of how different factors influence the physicochemical and folding properties of membrane-bound *c*-type cytochromes in general.

The ubihydroquinone:cytochrome *c* oxidoreductase (bc_1 complex)[1] is an enzyme encountered in a wide variety of organisms. This integral membrane protein is involved in both photosynthetic and respiratory electron transfer, and it contributes to the formation of an electrochemical gradient necessary for ATP synthesis. In prokaryotes, the bc_1 complex is composed of only three or four subunits, and is located within the cytoplasmic membrane (for reviews, see refs *1*−*4*). In eukaryotes, this enzyme is present in the inner mitochondrial membrane, and contains several additional subunits. A homologous complex is also found in chloroplast thylakoid membranes (called the b_6f complex), and transfers electrons between the two photosystems (for a review, see ref *5*). In all cases, this enzyme complex contains only three redox-active subunits which, in most bacteria, are encoded by genes organized as an operon called *pet* or *fbc* (for a review, see ref *4*). These subunits bear one *c*-type heme (cyt c_1), two *b*-type hemes (cyt b_{560} or b_H and cyt b_{566} or b_L), and one [2Fe-2S] iron sulfur cluster (Rieske Fe−S protein) as cofactors. Among them, the cyt *b* polypeptide is the main contributor of the two catalytic sites of the bc_1 complex. In bacterial cells, the Q_i site where ubiquinone reduction takes place is located on the cytoplasmic side of the membrane, and the Q_o site located on the periplasmic side is associated with ubihydroquinone oxidation.

Of special interest to this work is the cyt c_1 subunit which carries a single heme group covalently attached to the polypeptide chain by one (*6*) or, more frequently, two thioether bonds to cysteine residues. Various optical absorption, EPR, and MCD spectroscopic data indicate that the fifth and sixth axial ligands of cyt c_1 heme iron are usually histidine (H) and methionine (M), respectively (*7*−*9*; for a review, see ref *10*). Previous mutagenesis studies of the two highly conserved methionine residues located near the

† This work was supported by NIH Grant GM 38237 to F.D. and by Robert A. Welch Foundation Grant D-0710 to D.B.K.

* To whom correspondence should be addressed. Phone: (215) 898-4394. Fax: (215) 898-8780. E-mail: fdaldal@sas.upenn.edu.

‡ University of Pennsylvania.

§ TUBITAK.

|| Texas Tech University.

[1] Abbreviations: Bchl, bacteriochlorophyll; cyt, cytochrome; bc_1 complex, ubihydroquinone:cytochrome *c* oxidoreductase; b_H, high-potential *b*-type heme; b_L, low-potential *b*-type heme; b_6f complex, plastohydroquinone:plastocyanin oxidoreductase; DAD, 2,3,5,6-tetramethyl-1,4-phenylenediamine; DBH_2, 2,3-dimethoxy-5-decyl-6-methyl-1,4-benzohydroquinone; EDTA, ethylenediaminetetraacetic acid; TMBZ, tetramethylbenzidine; E_h, ambient potential; E_m, redox midpoint potential; E_{m7}, redox midpoint potential at pH 7; EPR, electron paramagnetic resonance; MCD, magnetic circular dichroism; MOPS, 3-(*N*-morpholino)propanesulfonic acid; PES, *N*-ethyl dibenzopyrazine ethosulfate; PMS, *N*-methyl dibenzopyrazine methosulfate; PMSF, phenylmethanesulfonyl fluoride; Ps, photosynthesis; Q_o, ubihydroquinone oxidation site; Q_i, ubiquinone reduction site; RC, reaction center; Res, respiration; RR, resonance Raman spectroscopy; SDS−PAGE, sodium dodecyl sulfate−polyacrylamide gel electrophoresis; SHE, standard hydrogen electrode; [2Fe-2S], two iron−two sulfur cluster.

10.1021/bi990211k CCC: $18.00
Published on Web 05/27/1999

carboxyl terminus of cyt c_1 revealed that in the facultative phototrophic bacterium *Rhodobacter capsulatus* M183 is the sixth axial ligand of cyt c_1 heme iron (*11*). Crystallographic data, now available for the mitochondrial bc_1 complex, are consistent with this assignment (*12*−*14*). In contrast to the situation with the bc_1 complex, in the chloroplast b_6f complex the sixth axial ligand of cyt *f* is provided by the free amino group of the amino terminal tyrosine residue (*15*).

In the case of *b*- and *c*-type cytochromes, several studies have used the four α-helix bundle structure of cyt b_{562} as a scaffold for the polypeptide chain (*16*), and the approach of semisynthesis as a means of generating natural and nonnatural ligands in cyt *c* (*17*, *18*). These studies have illustrated the influence of the sixth axial ligand on the properties of the heme group, and underlined its critical role in prosthetic group addition and polypeptide folding. On the other hand, very little work has been carried out on membrane-anchored *c*-type cytochromes such as the cyt c_1 subunit of the bc_1 complex, where proper incorporation of the mature hemoprotein into a multisubunit complex may be elaborate. Previously, only a few mutants affecting cyt c_1 in *Saccharomyces cerevisiae* (*19*), *R. capsulatus* (*11*), and *Rhodobacter sphaeroides* (*20*) have been studied. In particular, substitution of M183 with leucine (L) in the case of *R. capsulatus* yielded a cyt c_1 mutant with a drastically shifted E_{m7} value ($\Delta E_{m7} = -390$ mV), and an ability to bind CO, not observed with the wild-type protein. However, at least a subpopulation of this mutant cyt c_1 still exhibited spectroscopic properties characteristic of hexacoordinated heme. The possibility of another methionine residue acting as an axial ligand in the absence of M183 was ruled out by spectroscopic data (*9*), which in turn suggested a bis-histidine ligation for the M183L mutant cyt c_1. However, similar spectroscopic measurements also suggested that partial unfolding enhanced upon exposure to cryoprotectants could produce bis-histidine ligation in the case of the wild-type cyt c_1 as well (*9*). Thus, the nature of the sixth ligand in this cyt c_1 mutant lacking the natural M183 ligand remained unknown.

To further pursue our investigation on the role played by the sixth axial ligand in cyt c_1 heme−protein interactions, novel variants with possible histidine−lysine (K) or histidine−histidine (H) axial coordination were sought. For this purpose, the *R. capsulatus* cyt c_1 mutants M183K and M183H were constructed, and mutant bc_1 complexes were purified and characterized. It was found that both mutants incorporated heme into cyt c_1 but they yielded nonfunctional bc_1 complexes with unusual thermodynamic and spectroscopic properties. The availability of these stable cyt c_1 derivatives should now further our understanding of how the maturation and properties of cyt c_1 are affected by the chemical nature of its sixth axial ligand.

MATERIALS AND METHODS

Bacterial Strains and Growth. Escherichia coli and *R. capsulatus* strains were grown as described in ref *21* in the presence of appropriate antibiotics. Respiratory growth (Res) of *R. capsulatus* strains was achieved at 35 °C in the dark under semiaerobic conditions, and photosynthetic growth (Ps) at the same temperature under continuous light and anaerobic conditions. MT-RBC1 is a bc_1^- strain where the chromosomal copy of the *petABC* operon has been deleted and replaced by a gene cartridge conferring resistance to spectinomycin (*21*). The strain pMTS1/MT-RBC1 corresponds to MT-RBC1 complemented in trans with the plasmid pMTS1, which contains a wild-type copy of *petABC* and a kanamycin resistance cartridge. This strain, considered the wild-type reference strain in this study, overproduces the bc_1 complex by about 5−10-fold under Res growth conditions. The mutant strains pC:M183H/MT-RBC1 and pC:M183K/MT-RBC1 are identical to pMTS1/MT-RBC1, except that the codon corresponding to M183 of *petC* has been mutated to encode histidine and lysine, respectively.

Genetic Techniques. Site-directed mutagenesis was performed as described previously using uracilated DNA of phage M13mp10-BC1*Sma*del6 as a template (*11*), and the mutagenic oligonucleotides petC-M183H, 5′-TGG GCG CGC **CAC** CCC CCG CC-3′, and petC-M183K, 5′-TGG GCG CGC **AAG** CCC CCG CC-3′. After sequencing, appropriate DNA fragments bearing the desired mutation were exchanged with their wild-type counterparts in pMTS1 using the restriction enzymes *Sfu*I and *Stu*I, and yielded the plasmids pC:M183H and pC:M183K. These plasmids were then introduced into MT-RBC1 via triparental crosses (*21*).

Biochemical and Biophysical Techniques. Chromatophore membranes were prepared as described in ref *21* with a French pressure cell using a pressure of 18 000 psi, in MOPS buffer (50 mM, pH 7.0) containing 100 mM KCl, 1 mM EDTA, and 1 mM PMSF. They were washed three times in the same buffer without PMSF, and resuspended in the presence of 1 mM PMSF. Bacteriochlorophyll was extracted with 1 mL of ice-cold acetone/methanol (7/2 v/v) and its concentration determined spectrophotometrically using an ϵ_{775} of 75 mM^{-1} cm^{-1}. Purified bc_1 complexes were prepared as described in ref *22*, and protein concentrations were determined according to ref *23*. Sodium dodecyl sulfate−polyacrylamide gel electrophoresis (SDS−PAGE) was performed using an acrylamide concentration of 15%, and gels were stained with Coomassie blue for proteins, and with tetramethylbenzidine (TMBZ) for covalently attached hemes (*24*). Immunoblot analyses using monoclonal and polyclonal antibodies specific for the *R. capsulatus* bc_1 complex and DBH_2:cyt *c* reductase assays were performed as described in ref *21*.

Optical difference spectra for *b*- and *c*-type cytochromes were recorded using either a Hitachi U-3210 or a Shimadzu W2100U spectrophotometer. Samples were first oxidized by the addition of a small crystal of potassium ferricyanide, and then reduced by using either solid sodium ascorbate or sodium dithionite in the presence of 50 nM PMS. Protoheme and mesoheme contents were determined as described previously (*11*).

Flash-induced, single-turnover kinetics of cyt c_1 were performed as described in ref *25* using chromatophore membranes and a single-wavelength spectrophotometer (Biomedical Instrumentation Group, University of Pennsylvania, Philadelphia, PA) in the presence of 2.5 μM valinomycin, 2.5 μM PMS, 2.5 μM PES, 8 μM DAD, 10 μM 2-hydroxy-1,4-naphthoquinone, and 10 μM $FeCl_3$−EDTA. The quantity of chromatophore membranes used in the assay corresponded to 0.1−0.15 μM reaction center (RC), whose concentration was determined by measuring the optical absorbance difference between 605 and 540 nm at an E_h of 380 mV, and using an extinction coefficient of 29.8 mM^{-1}

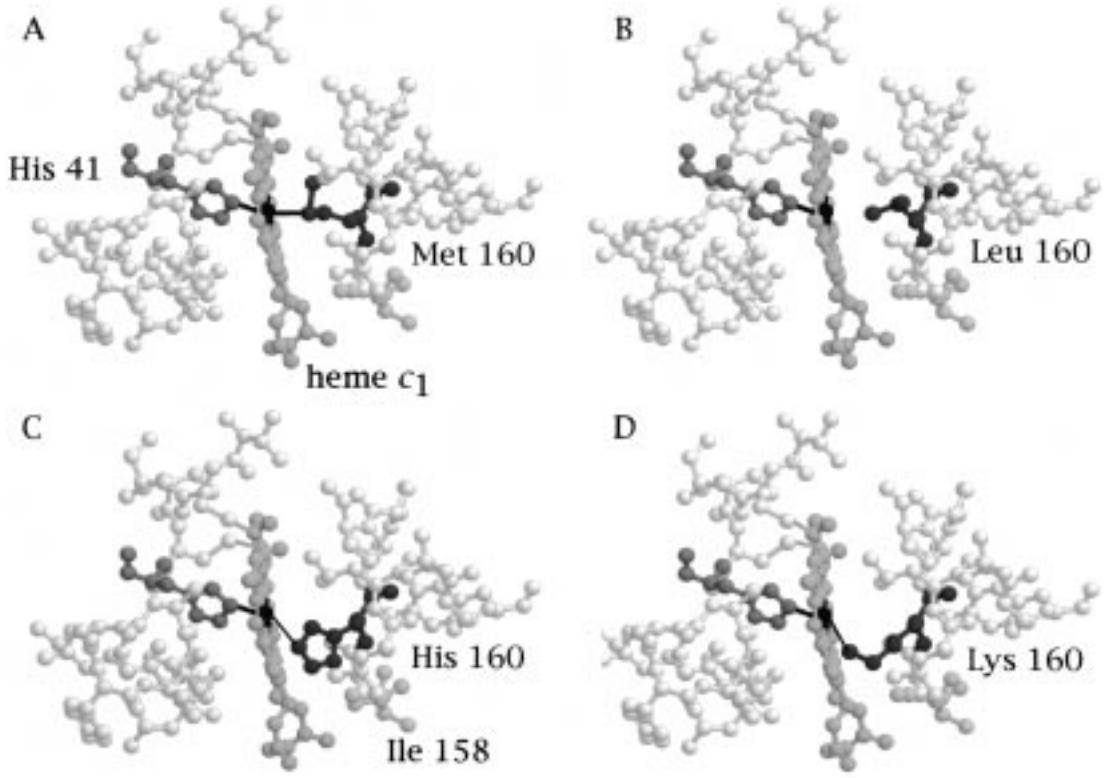

FIGURE 1: Heme binding region of the cyt c_1 subunit of the bc_1 complex. The figure is for depicting a hypothetical three-dimensional structure of cyt c_1 mutants using the coordinates of the bovine heart mitochondrial bc_1 complex. Panels A−D depict the wild type (M160) and M160L, M160H, and M160K cyt c_1 mutants corresponding to *R. capsulatus* M183 wild type and M183L, M183H, and M183K mutants, respectively. The residues surrounding heme (within a radius of 8−10 Å from iron) are shown in light gray, and a slightly darker gray tone was used for the isoleucine 158 side chain (for further details, see the text). The fifth ligand histidine 41 (histidine 38 in *R. capsulatus*), and the different amino acid residues at position 160 (position 183 in *R. capsulatus*) which provide the sixth ligand, are shown in dark gray. The coordination between histidine 41 (or methionine 160), and the possible coordination between the histidine (in M183H), or lysine (in M183K) and the iron atom of heme is represented by thick and thin black lines, respectively.

cm^{-1}. Transient cyt *c* re-reduction kinetics initiated by a short saturating flash (8 μs) from a xenon lamp were followed at 550−540 nm.

Dark equilibrium redox titrations of the heme groups were performed as described in ref *26*. Chromatophore membranes (10−12 mg in 8 mL corresponding to approximately 20 μM Bchl), or the purified bc_1 complex (1.2 mg of protein in 8 mL), in MOPS buffer (50 mM, pH 7.0) containing 100 mM KCl were incubated in the presence of 20 μM PMS, 20 μM PES, 50 μM DAD, and 25 μM 2-hydroxy-1,4-naphthoquinone, 1,4-naphthoquinone, and 1,2-naphthoquinone. Titrations were performed in the α-band region, and the E_m values were determined by fitting the data to an $n = 1$ (or two $n = 1$, if appropriate) Nerst equation, as described previously (*25*). When the E_m values of cytochromes b_H, b_L, and c_1 were too close to each other, it was not possible to titrate them independently since their α peaks also overlap partially, and their deconvolution was necessary for accurate titrations. For this purpose, the contribution of the symmetric point on the *b* peak (around 570 nm) was subtracted from the value of cyt c_1 (around 550 nm). In addition, when needed, the difference 590−540 nm value was used to estimate the shift of the baseline which often occurs below −100 mV. Processing the data in this fashion was satisfactory when only the cyt b_H peak interfered, since it is highly symmetrical. However, when the contribution of cyt b_L was prominent, then this approach became unsatisfactory as the *b* peak broadens due to the split spectrum of cyt b_L (*22*). A more elaborate Lorentzian deconvolution with two components was also used, and yielded similar results (data not shown). To what extent the slight deviation of the titration curves from an $n = 1$ behavior observed in some cases is due to data processing or to other factors is unclear. In any event, because of the extensive data processing, the E_{m7} values presented in this work should be considered approximate, and are only given for comparison purposes.

Molecular modeling was carried out using the program Swiss-Pdb Viewer written by N. Guex and M. C. Peitsch (http://www.pdb.bnl.gov/expasy/spdbv/mainpage.htm). The coordinates of the bovine heart mitochondrial bc_1 complex (1BE3, kindly provided by S. Iwata prior to their release in the Protein Data Bank) were used. The liganding methionine was first mutated to H or K; the different possible rotamers were analyzed, and the rotamer with the most favorable distance and angle for heme iron ligation was chosen. In case of clashes with another amino acid residue, a different rotamer for the latter residue was searched. After modeling, the coordinates were visualized using the Rasmol program written by R. Sayle (http://www.umass.edu/microbio/rasmol/).

Chemicals. All chemicals were as described previously (*27*).

RESULTS

Choice and Construction of the M183H and M183K Mutants. The purpose of this study was to further pursue our investigations of the role played by the sixth axial ligand in heme−protein interactions in the case of cyt c_1, and also

Table 1: Various Properties of *R. capsulatus* Cyt c_1 Sixth Axial Ligand Mutants

		bc_1 activity		properties of cyt c_1 heme[b]	
strain	phenotype[a]	DBH_2[c] (%)	flash kinetics[d] (%)	E_{m7} (mV)	λ_{max} (nm)
wild-type	Ps^+	100	100	310−340	551−552
MT-RBC1	Ps^-	0.5	0		
M183H	Ps^-	0.5	1.5	30−50 and ∼−140	552−554
M183K	Ps^-	2	0	60−80	548−549
M183L[e]	Ps^-	1.5	nd[f]	−74	551

[a] Ps^+ and Ps^- represent the ability and inability, respectively, to grow photosynthetically on MPYE plates at 35 °C. [b] Properties of the cyt c_1 heme group in chromatophore membranes and purified bc_1 complexes. [c] DBH_2 cyt *c* oxidoreductase activity (percentage of the wild-type activity which in this particular instance was about 4000 nmol of cyt *c* reduced min^{-1} mg of membrane $protein^{-1}$). [d] Transient cyt *c* re-reduction kinetics after flash-induced oxidation (percentage of the wild-type rate which in this particular instance was 290 s^{-1}). [e] The data for the M183L mutant were taken from ref *11*. [f] nd, not determined.

to shed light on the nature of the amino acid residue acting as the sixth axial ligand in the M183L mutant (*9*). As the only other amino acid residues with a ligand field strength sufficient enough to yield a low-spin state heme iron are histidine, lysine, and cysteine, and our earlier spectroscopic investigations of the M183L mutant indicated the presence of a nitrogen-containing sixth ligand (*9*), the M183H and M183K substitutions were most interesting. In this respect, it is noteworthy that in the chloroplast b_6f complex the sixth axial ligand of cyt *f* is the amino group of the amino terminal tyrosine residue, and in mitochondrial cyt *c*, histidine−lysine ligation seems to be present in the protein at alkaline pH values (*28*).

Molecular modeling attempts using the coordinates from the bovine heart mitochondrial bc_1 complex indicated that substitution of M160 (corresponding to M183 in *R. capsulatus*) with histidine or lysine could still allow the proper coordination of an appropriate nitrogen atom to the heme iron without perturbing drastically the protein backbone (Figure 1). In the case of H160 (H183 in *R. capsulatus*) substitution, provided that the side chain of isoleucine 158 (alanine 181 in *R. capsulatus*) was rearranged, a rotamer could be found for which the distance (2.6 Å) and angle (150°) between the ϵ-N of histidine and heme iron were within the range (1.8−2.7 Å and 150−180°) encountered in other bis-histidine ligated cytochromes. Rotamers with similar properties were also observed with K160 (K183 in *R. capsulatus*) substitution, but due to lack of data in the case of histidine−lysine coordination, a similar comparison was not possible.

Growth and Cyt c Reductase Activities of the Mutants. The mutants M183H and M183K, like M183L (*11*), were unable to support the Ps growth of *R. capsulatus*, suggesting that they had no bc_1 complex activity. The deleterious effect of these mutations on the bc_1 complex was then investigated by monitoring the DBH_2:cyt *c* reductase activity, and light-induced transient cyt *c* re-reduction kinetics using chromatophore membranes. The results, summarized in Table 1, demonstrated that no steady-state, or single turnover, bc_1 complex activity was detectable in either of the mutants.

Assembly and Heme Content of Mutant bc_1 Complexes. In yeast, it is known that mutation of the sixth axial ligand

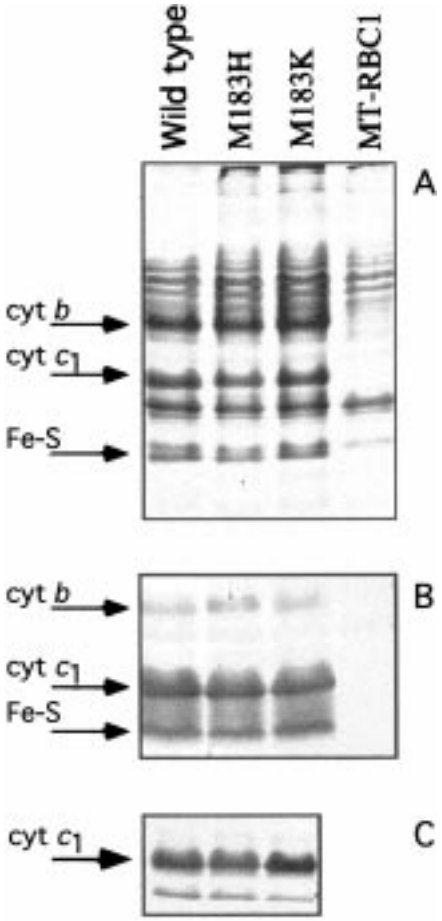

FIGURE 2: SDS−PAGE and Western blot analyses of chromatophore membranes. Acrylamide gels (15%) were stained for proteins with Coomassie blue (A) and for heme with TMBZ (C) and immunoprobed using monoclonal antibodies against *b* and c_1 subunits and polyclonal antibodies against the Fe−S subunit after blotting into a membrane (B). Sixty micrograms of membranes proteins was loaded per lane.

methionine of cyt c_1 to leucine interferes with the covalent attachment of heme, and leads to the accumulation of its precursor form (*19*). Thus, it seemed important to determine whether the lack of the bc_1 complex activity in *R. capsulatus* M183H or M183K mutants was due to the absence of a properly assembled bc_1 complex. SDS−PAGE, immunoblot, and TMBZ staining data obtained using chromatophore membranes revealed that the heme group was covalently attached to cyt c_1, which in turn was assembled properly into the bc_1 complex in both M183H and M183K mutants (Figure 2), yielding stable cyt c_1 mutants.

Redox Optical Difference Spectroscopy. Optical difference spectroscopy was used to estimate the amounts of *b*- and *c*-type hemes present in chromatophore membranes so the fraction associated with the bc_1 complex could be deduced. The spectra obtained after ascorbate or dithionite reduction of appropriate *R. capsulatus* mutants are shown in Figure 3. Dithionite minus ferricyanide difference spectra (Figure 3B) revealed that all mutants contained *b*- and *c*-type cytochromes (α peaks around 550 and 560 nm). On the other hand, ascorbate minus ferricyanide spectra (Figure 3A) indicated that unlike the wild-type spectrum (d), no peak at 550 nm could be detected in the difference spectrum of the M183H mutant (b), and that only a small feature with a maximum at 550 nm was seen in that of the M183K mutant (c). These

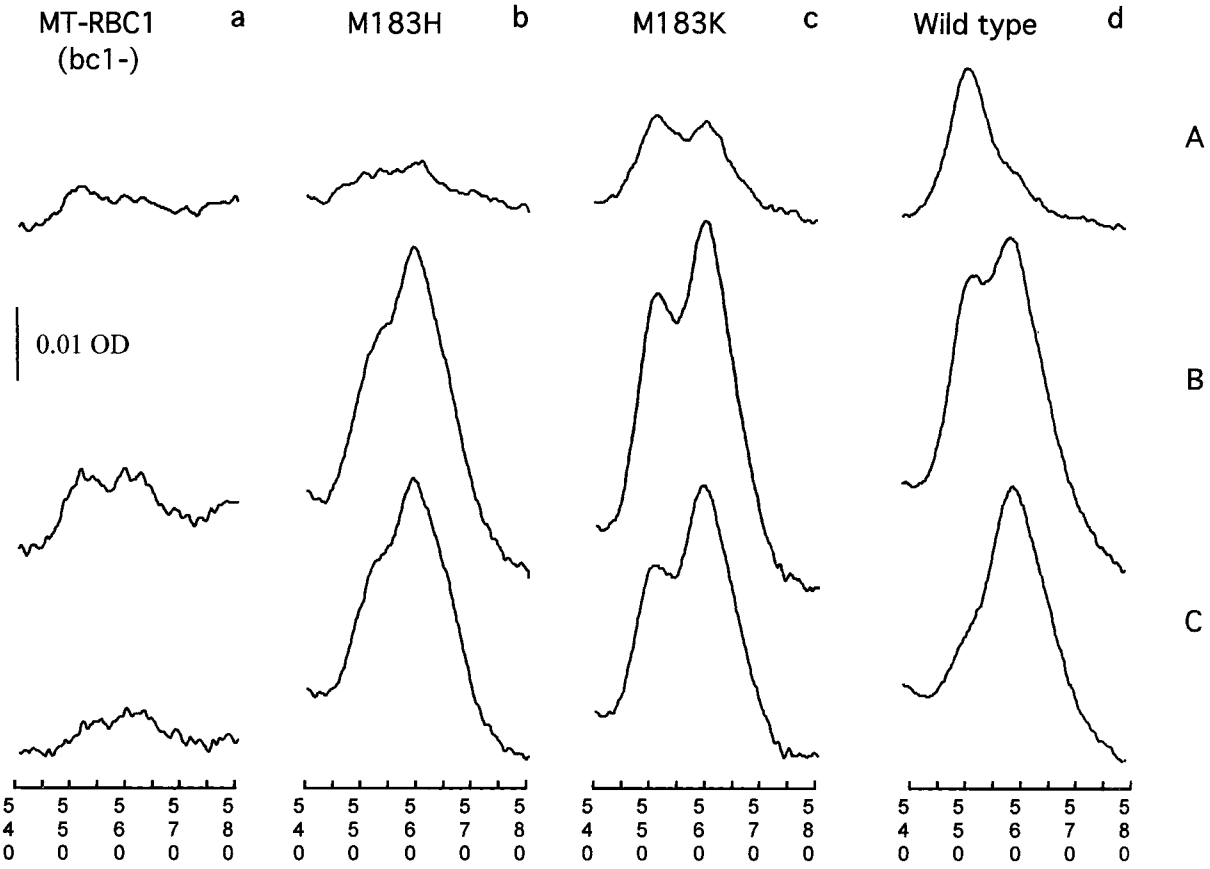

FIGURE 3: Reduced minus oxidized difference spectra of various strains. Chromatophore membranes (0.8 mg of proteins/mL) were suspended in 50 mM MOPS (pH 7.0) containing 100 mM KCl and 50 nM PMS. The spectra in panel A were obtained by subtracting the ferricyanide-oxidized spectra from the ascorbate-reduced spectra. The spectra in panel B were obtained by subtracting the ferricyanide-oxidized spectra from the dithionite-reduced spectra. The spectra in panel C (dithionite minus ascorbate) were obtained by mathematically subtracting the spectra in panel A from those in panel B. In each case, traces a to d correspond to MT-RBC1, M183H, M183K, and the wild type (pMTS1/MT-RBC1), respectively.

data suggested that, as in the case of the M183L mutant (*11*), modification of the sixth axial ligand also decreased the E_m value of cyt c_1 in these mutants. Moreover, the partial reduction of cyt c_1 by ascorbate observed for M183K suggested that in the latter mutant this E_m value must be higher than those of M183H and M183L mutants (*11*), and was probably above 0 mV.

Dark Equilibrium Redox Titrations. Because the nature of the heme axial ligand is considered an important component influencing the E_m value of a heme group (*10*), dark equilibrium redox titrations were performed. These experiments also enabled us to demonstrate that the E_{m7} values of the *b*-type hemes of the bc_1 complex were not altered in the mutants (data not shown). Data obtained using the wild-type (Figure 4A) and mutant (data not shown) chromatophore membranes revealed that a component with an E_{m7} value of ~300 mV was present in all cases, and corresponded to various *c*-type cytochromes. In the mutants, titrations of cyt c_1 without interference from contribution by cyts b_H and b_L became particularly difficult due to their similar E_{m7} values and overlapping α peaks. Thus, an approximate approach for deconvoluting these peaks, as described in Materials and Methods, was adopted for processing the data (Figure 4). In the case of the M183H mutant, the titration curve obtained between 0 and −200 mV suggested the presence of a component absorbing around 550 nm and titrating in this E_h range (Figure 4D). Careful examination of the optical difference spectra between −200 and −150 mV indicated that this component, which overlapped with the cyt b_L peak, was present only in the M183H mutant and not in M183K or the wild-type strains (Figure 5C), and was also not an artifact due to baseline shifts. Moreover, in the M183H mutant, yet another cyt c_1 species with an E_{m7} value of ~30 mV (Figure 4C) appeared as a shoulder on the cyt *b* peak (Figure 5D). The optical difference spectrum between −50 and 0 mV revealed a λ_{max} of ~554 nm for this latter component, but due to the contribution from the cyt *b* peak, it was impossible to assign a precise λ_{max} value to it (Figure 5D). On the other hand, cyt c_1 of the M183K mutant was almost completely reduced around 0 mV (Figure 4B), and exhibited an α peak centered around 548−549 nm (Figure 5A). The novel features of the M183H and M183K mutants, which differ from those of the wild-type cyt c_1 (a λ_{max} of ~552 nm and an E_{m7} of ~300 mV) (*11*), are summarized in Table 1.

Analyses of Purified Mutant bc_1 Complexes. When the fact that chromatophore membranes contain many different *b*- and *c*-type cytochromes is considered, full characterization of the mutant bc_1 complexes required their purification to homogeneity. SDS−PAGE, immunoblot, and TMBZ staining data obtained using proteins purified as described in Materials and Methods indicated that the mutant bc_1 complexes were stable, and their properties were not altered drastically upon detergent solubilization and purification. Minor heme stain-

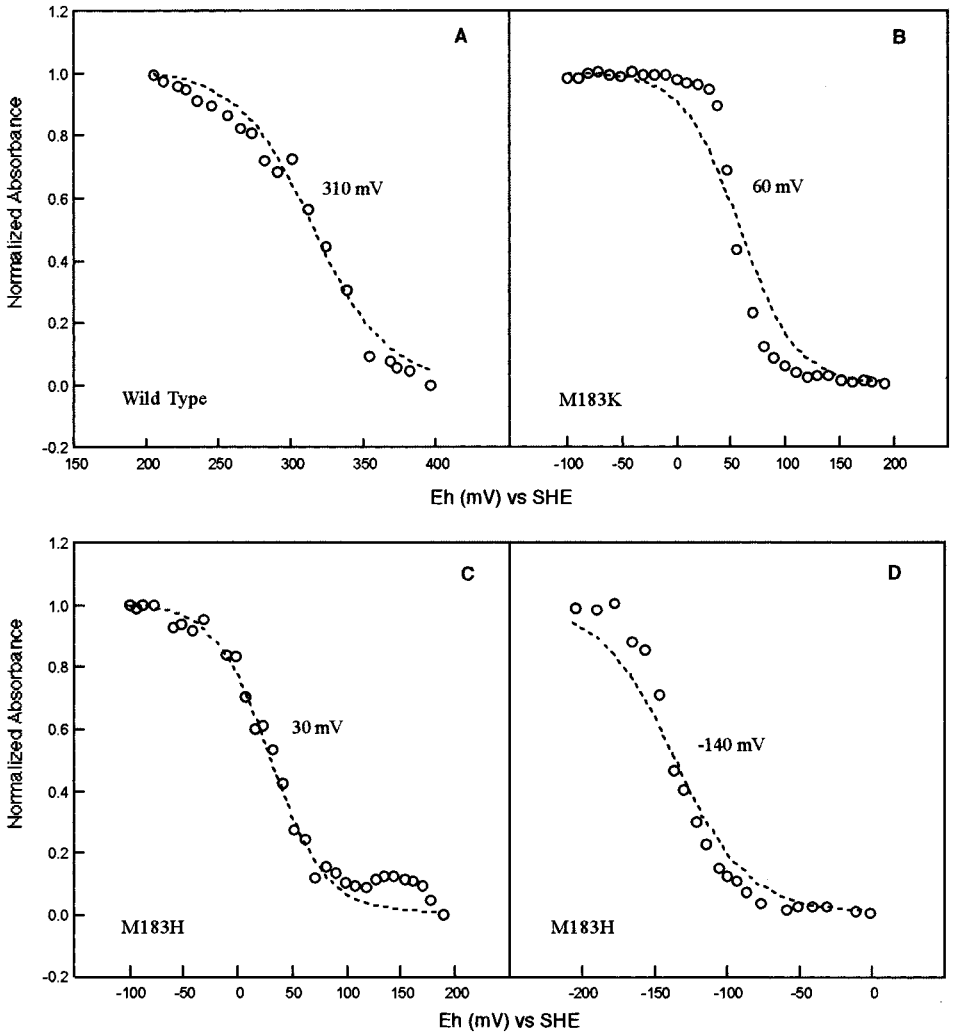

FIGURE 4: Redox titration of various chromatophore membranes. Reductive dark equilibrium redox titrations were performed, and the data were processed, as described in Materials and Methods: (A) pMTS1/MT-RBC1 (wild type) monitored at 550−540 nm, (B) the M183K mutant monitored at 549−570 nm, (C) the M183H mutant (higher-potential component) monitored at 552−570 nm, and (D) the M183H mutant (lower-potential component) monitored at 552−570 nm *minus* that at 590−540 nm.

able bands, noted especially in the case of the M183H mutant, were attributed to proteolytic degradation products of cyt c_1 (data not shown), as previously seen with M183L (*11*). To further confirm the proper assembly of the mutant bc_1 complexes, the protoheme/mesoheme ratio was determined using purified samples, and a stoichiometry of 2.0 ± 0.1 was found in all cases. As expected, the purified bc_1 complexes containing the M183H and M183K mutations exhibited no detectable cyt *c* reductase activity.

Optical redox difference spectra of purified bc_1 complexes gave a first indication about the heme spin state of cyt c_1 in various mutants. In contrast to a reduced high-spin *c*-type heme which has a Sorét transition shifted toward 430 nm and a broad $\alpha-\beta$ region, both the M183H and M183K mutants of cyt c_1 exhibited sharp α and β bands (Figure 6), and sharp and intense Sorét transitions (not shown). In a wild-type bc_1 complex, the features observed in an ascorbate minus ferricyanide difference spectrum can be attributed to cyt c_1 only with α and β band maxima at 552 and 523 nm, respectively (Figure 6A). However, the α bands of the M183H (Figure 6B) and M183K (Figure 6C) cyt c_1 mutants appear as a shoulder (M183H), or a peak (M183K), around 550 nm in the dithionite minus ferricyanide difference spectra, which also feature the 560 nm maximum for cyts b_H and b_L. Although the reduced spectra could only be obtained after addition of dithionite, as mentioned above for spectra obtained with chromatophore membranes and hence including the transitions of both *b*- and *c*-type hemes, their sharpness suggested that at least a subpopulation of M183H and of M183K cyt c_1 mutants also had a hexacoordinate low-spin heme.

Dark equilibrium redox titrations (Figure 7) performed using purified bc_1 complexes further indicated that the E_{m7} values of the heme groups were similar to those obtained using chromatophore membranes (Figure 4). In particular, the optical difference spectra shown in Figure 8 were like those obtained using chromatophore membranes (Figure 5), and the presence of two cyt c_1 subpopulations with different E_m values in the case of M183H were discernible (Figures 7 and 8C,D). To test whether these two subpopulations were due to a partial dissociation of the histidine ligand at pH 7.0, similar measurements were also repeated at pH 11.0, and revealed that at least the species exhibiting a high E_m value was still present under these conditions. Further characterization of the two forms of cyt c_1 in M183H should await isolation of this subunit, which is in progress.

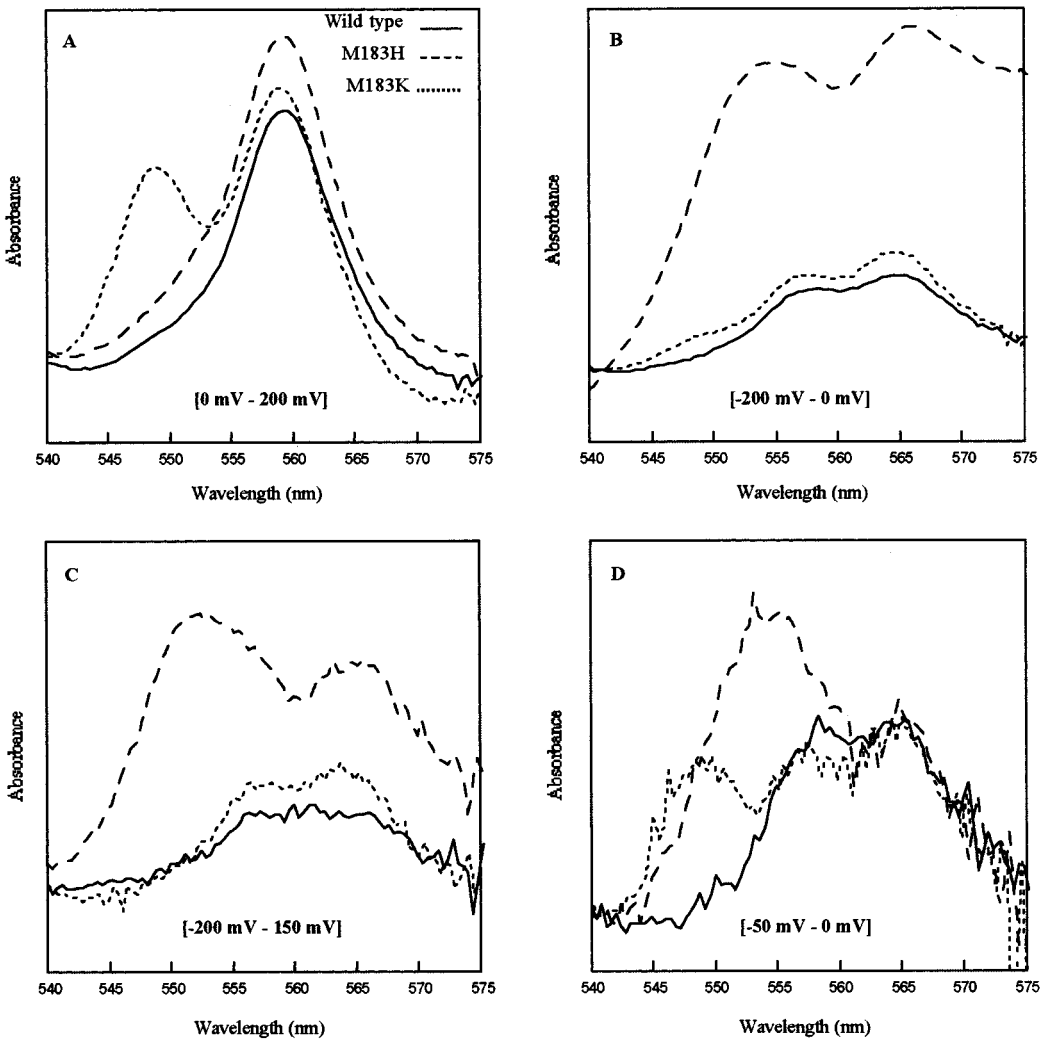

FIGURE 5: Optical difference spectra of various chromatophore membranes. The initial spectra were recorded during reductive dark equilibrium redox titrations, and the difference spectra were obtained by choosing appropriate E_h values. —, - - -, and — — — correspond to the wild type, M183H, and M183K, respectively: (A) 0 to 200 mV range: wild type (0 *minus* 189 mV), M183H (−2 *minus* 189 mV), and M183K (0 *minus* 191 mV); (B) −200 to 0 mV range: wild type (−200 *minus* 0 mV), M183H (−205 *minus* −2 mV), and M183K (−200 *minus* 0 mV); (C) −200 to −150 mV range: wild type (−200 *minus* −150 mV), M183H (−205 *minus* −157 mV), and M183K (−200 *minus* −152 mV); and (D) −50 to 0 mV range: wild type (−54 *minus* 0 mV), M183H (−52 *minus* −2 mV), and M183K (−51 *minus* 0 mV). For each panel, the absorbance scale (not shown) was chosen to illustrate best the difference spectra, so their amplitudes are not directly comparable.

DISCUSSION

In this study, a detailed investigation of the role played by the sixth axial ligand in the case of the cyt c_1 subunit of the bc_1 complex was performed using two novel *R. capsulatus* cyt c_1 mutants in which the native sixth axial ligand M183 was replaced with a histidine or a lysine, via site-directed mutagenesis. This approach is distinct from studies using soluble cyt *c* which attempt to deduce the influence of heme environment on the physicochemical properties of this redox group by comparing cytochromes from various species, where many parameters change at once, and may allow a better correlation of the structural changes and their functional consequences.

Decrease of the E_{m7} values of about 250 and 300 for the M183K and M183H mutants, respectively, are not unexpected in light of our earlier work with M183L, where an even more drastic change has been observed (*11*). However, it should be noted that the extent of the ΔE_{m7} changes could not be predicted before these studies. These findings further corroborate the importance of the molecular nature of the sixth axial ligand in controlling the E_m value of the heme group in cyt c_1, and are in agreement with the electronic properties of the different ligands. Indeed, the sulfur atom of methionine is a good π electron acceptor; thus, it preferentially stabilizes the reduced state, and consequently increases the E_m value. Studies with model systems have indicated that coordination by imidazole of the heme Fe atom decreases its E_m value by about 150 mV as compared to sulfur coordination (*29*, *30*). In addition, the E_{m7} values of natural *c*-type hemes with histidine−methionine ligation range from 0 to 400 mV, whereas those with bis-histidine ligation have lower values, often in the range of −400 to −100 mV (*10*).

The use of semisynthesis to generate various natural and non-natural ligands in mitochondrial cyt *c* (*17*) has revealed similar features for a histidine ligand with a decrease of the E_{m7} value of about 230 mV. Similarly, substitution of the methionine ligand of cyt c_{550} from *Thiobacillus versutus* with a lysine also decreased its E_{m7} value by about −330 mV (*31*). On the other hand, the E_{m7} value of cyt *f*, which belongs

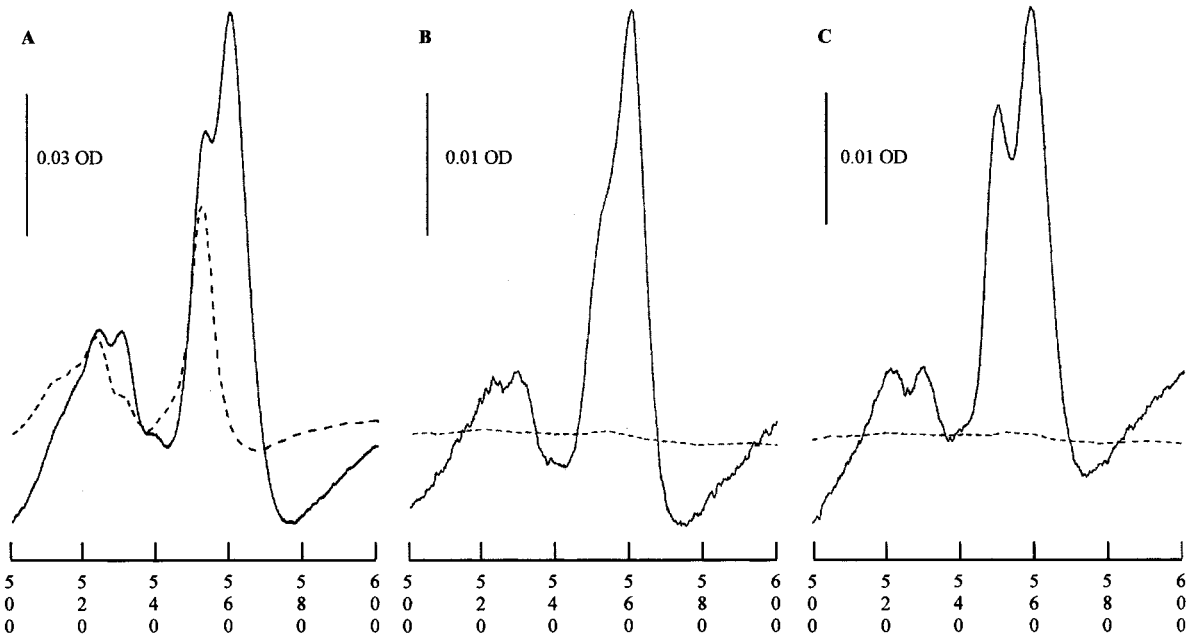

FIGURE 6: Optical difference spectra of purified bc_1 complexes: (A) wild-type bc_1 complex (2.5 μM), (B) M183H (0.9 μM), and (C) M183K (0.8 μM). Spectra were obtained using samples dissolved in 50 mM Tris-HCl buffer (pH 8.0) containing 100 mM NaCl and 0.1 mg/mL dodecyl maltoside in a cuvette with a 1 cm optical path length. — and - - - correspond to dithionite minus ferricyanide and ascorbate minus ferricyanide spectra, respectively.

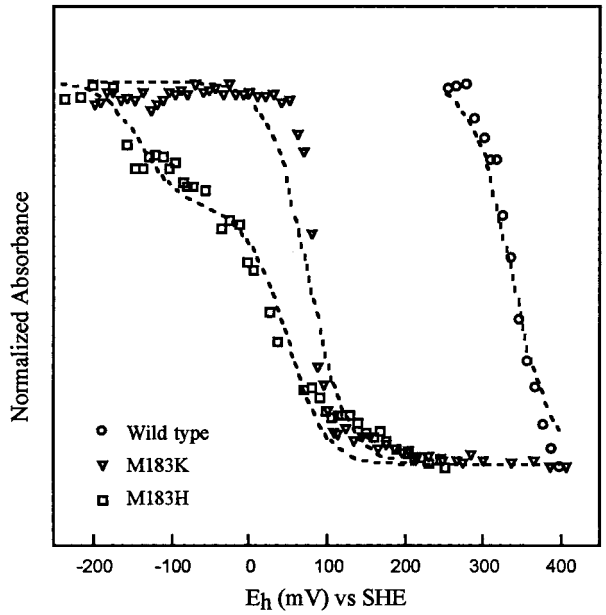

FIGURE 7: Redox titration of purified bc_1 complexes. Reductive dark equilibrium redox titrations were performed, and the data fitted, as described in Materials and Methods. ○, □, and ▽ correspond to pMTS1/MT-RBC1 (wild-type bc_1 complex) monitored at 550−540 nm, the M183H mutant monitored at 553−568 nm, and the M183K mutant monitored at 549−570 nm, respectively.

to a different structural class of *c*-type cytochrome, is rather high (330−370 mV) (*5*). However, to what extent the electronic properties of the nitrogen atom of a free amino terminal residue are different from that of the ϵ-amino group of a lysine residue is unknown. Thus, the mutations studied here are not to be compared with cyt *f* nor are intended to mimic a cyt *f*-like cyt c_1. Finally, it should be noted that the nature of the axial ligand is not the only parameter influencing the redox properties of a heme group. Additional factors, including solvent exposure, surface charge, internal dielectric constant, hydrophobicity, electrostatic interaction, and structural constraints, may be very different among various cytochromes with similar bis-nitrogen axial ligation (*10*).

The mutations analyzed here shifted the position of the α band toward shorter and longer wavelengths for M183K and M183H mutants, respectively. A similar red shift has also been observed in the case of a cyt *c* mutant with a histidine ligand instead of methionine (*17*). This change in the energy transition level between the bonding (π) and antibonding (π^*) molecular orbital of the porphyrin ring is probably due to the direct effect of the liganding atom (N vs S) on the electronegativity of the Fe atom. More detailed spectroscopic studies, to be performed using purified mutant cyt c_1 subunits, should further define the nature of the ligands as well as the influence of these mutations on the electronic properties of cyt c_1 heme.

The mutants obtained during this work demonstrated that covalent attachment of the heme prosthetic group to the cyt c_1 apoprotein and assembly of this subunit into the bc_1 complex are not abolished in *R. capsulatus* (*11*). The nature of the sixth axial ligand is not crucial for these processes, which is in contrast with the yeast cyt c_1 case, where a leucine variant does not assemble the cyt c_1 subunit, and a lysine variant does so poorly (*19*). Whether this is due to a higher stability of *R. capsulatus* cyt c_1, or to the different folding and assembly processes in bacteria and mitochondria, is unknown. In any event, the availability of the stable cyt c_1 mutants described here should now render possible further studies on the ligand properties of hemoproteins.

Mitochondrial cyt *c* undergoes ligand switching during its folding process from a bis-histidine (thought to involve as a sixth ligand His 26 or His 33 in this case) to a histidine−water (a pentacoordinated ligation state) and then to its final histidine−methionine ligated form (*32*, *33*). The folding pathway for a membrane-attached *c*-type cytochrome such as cyt c_1 has not been studied. If that of *R. capsulatus*

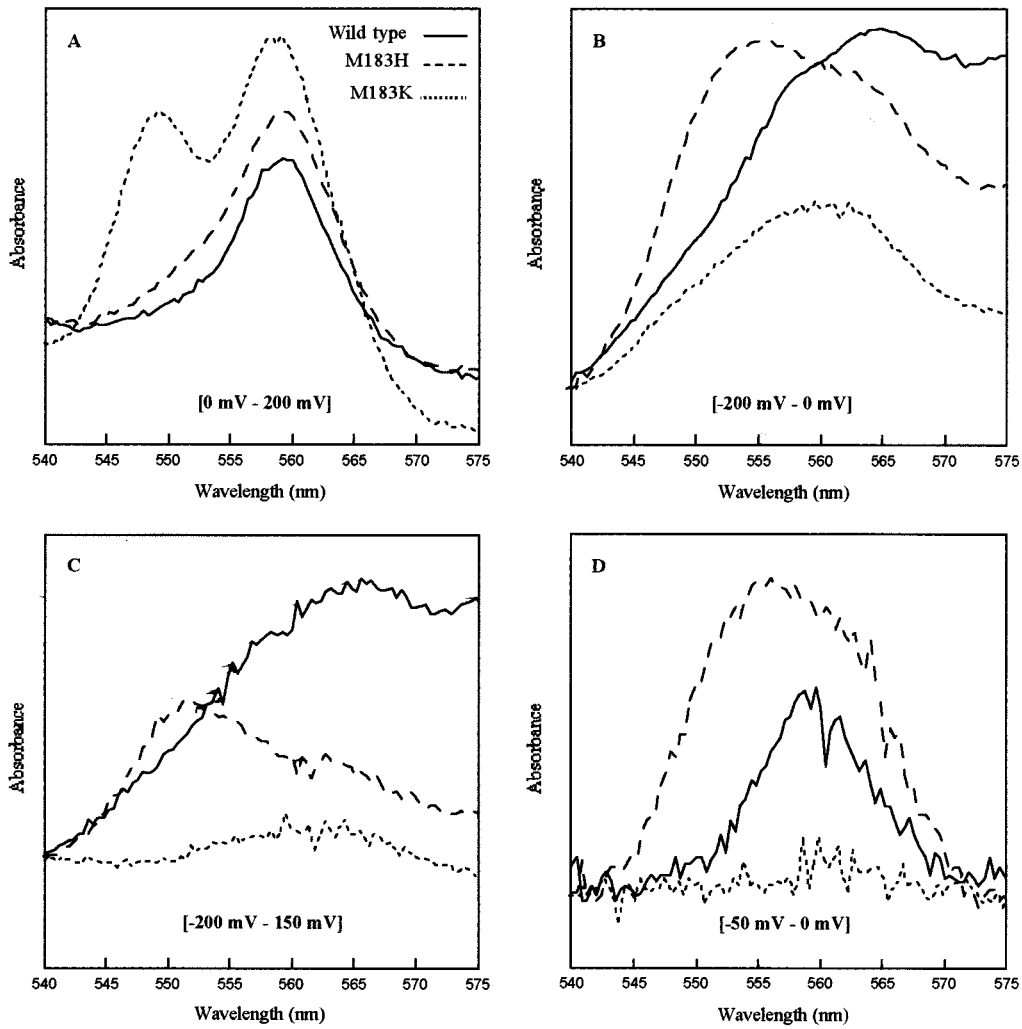

FIGURE 8: Optical difference spectra of various bc_1 complexes. The initial spectra were recorded during reductive dark equilibrium redox titration, and the difference spectra were obtained by choosing specific E_h values. —, - - -, and — — — correspond to the wild type, M183H, and M183K, respectively: (A) 0 to 200 mV range: wild type (0 *minus* 200 mV), M183H (−4 *minus* 204 mV), and M183K (0 *minus* 205 mV); (B) −200 to 0 mV range: wild type (−202 *minus* 0 mV), M183H (−203 *minus* −4 mV), and M183K (−201 *minus* 0 mV); (C) −200 to −150 mV range: wild type (−202 *minus* −152 mV), M183H (−203 *minus* −150 mV), and M183K (−201 *minus* −149 mV); and (D) −50 to 0 mV range: wild type (−50 *minus* 0 mV), M183H (−59 *minus* −4 mV), and M183K (−53 *minus* 0 mV). For the absorbance scale, see the legend of Figure 5.

involves a similar mechanism, then the two species with different E_m values observed in the case of the M183H mutant may correspond to an equilibrium between a bis-histidine folding intermediate (possibly involving as a sixth axial ligand either His 7 or His 177 of *R. capsulatus* cyt c_1) and a bis-histidine folded state involving His 38 and His 183. Interestingly, Finnegan et al. (*9*) have already noticed the presence of two different forms of cyt c_1 when purified preparations of the wild type and M183L mutant of *R. capsulatus* (*11*) were exposed to cryoprotectants such as ethylene glycol, and noted that this feature was greatly enhanced in the case of bacterial cytochromes c_1. The observation of two subpopulations with M183H mutant cyt c_1 might allow us to further characterize the different species, and define their molecular natures.

In summary, this work demonstrated that substitution of the methionine sixth axial ligand of cyt c_1 heme iron with either a histidine or a lysine yields stable mutant proteins with different physicochemical properties with respect to their E_{m7} and λ_{max} values, which are also different from those of the M183L mutant, described previously (*11*). Considering that purified mutant bc_1 complexes are stable, we are hopeful that purification of the mutant cyt c_1 subunits would allow further determination of their physicochemical properties and definition of the molecular identity of their heme iron axial ligands.

ACKNOWLEDGMENT

We thank A. Sami Saribas for verification of the nucleotide sequence of the mutations after mutagenesis, Maria Valkova-Valchanova for her gift of the purified wild-type bc_1 complex, Nurjana Bachman for help with mutagenesis, and Masakazu Hirasawa for assistance with purification and redox spectra of the isolated mutant bc_1 complexes.

REFERENCES

1. Knaff, D. B. (1993) *Photosynth. Res. 35*, 117−133.
2. Gennis, R. B., Barquera, B., Hacker, B., Van, D. S. R., Arnaud, S., Crofts, A. R., Davidson, E., Gray, K. A., and Daldal, F. (1993) *J. Bioenerg. Biomembr. 25*, 195−209.
3. Brandt, U., and Trumpower, B. (1994) *Crit. Rev. Biochem. Mol. Biol. 29*, 165−197.
4. Gray, K. A., and Daldal, F. (1995) in *Anoxygenic Photosynthetic Bacteria* (Blankenship, R. E., Madigan, M. T., and

Bauer, C., Eds.) pp 747−774, Kluwer Academic Publishers, Dordrecht, The Netherlands.
5. Cramer, W., Soriano, G., Ponomarev, M., Huang, D., Zhang, H., Martinez, S., and Smith, J. (1996) *Annu. Rev. Plant Physiol. 47*, 477−508.
6. Mukai, K., Yoshida, M., Toyosaki, H., Wakabayashi, S., and Matsubara, H. (1989) *Eur. J. Biochem. 178*, 649−656.
7. Simpkin, D., Palmer, G., Devlin, F. J., McKenna, M. C., Jensen, G. M., and Stephens, P. J. (1989) *Biochemistry 28*, 8033−8039.
8. Lou, B.-S., Hobbs, J. D., Chen, Y.-R., Yu, L., Yu, C.-A., and Ondrias, M. R (1993) *Biochim. Biophys. Acta 1144*, 403−410.
9. Finnegan, M. G., Knaff, D. B., Qin, H., Gray, K. A., Daldal, F., Yu, L., Yu, C.-A., Kleis-San Francisco, S., and Johnson, M. K. (1996) *Biochim. Biophys. Acta 1274*, 9−20.
10. Moore, G. R., and Pettigrew, G. W. (1990) in *Cytochromes c. Evolutionary, structural and physicochemical aspects*, Springer Series in Molecular Biology, Springer-Verlag, Berlin and Heidelberg, Germany.
11. Gray, K. A., Davidson, E., and Daldal, F. (1992) *Biochemistry 31*, 11864−11873.
12. Xia, D., Yu, C.-A., Kim, H., Xia, J. Z., Kachurin, A. M., Zhang, L., Yu, L., and Deisenhofer, J. (1997) *Science 277*, 60−66.
13. Zhang, Z., Huang, L., Shulmeister, V. M., Chi, Y.-I., Kim, K. K., Hung, L.-W., Crofts, A. R., Berry, E. A., and Kim, S.-H. (1998) *Nature 392*, 677−684.
14. Iwata, S., Lee, J. W., Okada, K., Lee, J. K., Iwata, M., Rasmussen, B., Link, T. A., Ramaswamy, S., and Jap, B. K. (1998) *Science 281*, 64−71.
15. Martinez, S. E., Huang, D., Szczepaniak, A., Cramer, W. A., and Smith, J. L. (1994) *Structure 2*, 95−105.
16. Barker, P. D., Nerou, E. P., Cheesman, M. R., Thomson, A. J., de Oliveira, P., and Hill, H. A. O. (1996) *Biochemistry 35*, 13618−13626.
17. Wallace, C. J. A., and Clark-Lewis, I. (1992) *J. Biol. Chem. 267*, 3852−3861.
18. Raphael, A. L., and Gray, H. B. (1989) *Proteins 6*, 338−340.
19. Nakai, M., Ishiwatari, H., Asada, A., Bogaki, M., Kawai, K., Tanaka, Y., and Matsubara, H. (1990) *J. Biochem. 108*, 798−803.
20. Konishi, K., Van Doren, S. R., Kramer, D. M., Crofts, A. R., and Gennis, R. B. (1991) *J. Biol. Chem. 266*, 14270−14276.
21. Atta-Asafo-Adjei, E., and Daldal, F. (1991) *Proc. Natl. Acad. Sci. U.S.A. 88*, 492−496.
22. Robertson, D. E., Ding, H., Chelminski, P. R., Slaughter, C., Hsu, J., Moomaw, C., Tokito, M., Daldal, F., and Dutton, P. L. (1993) *Biochemsitry 32*, 1310−1317.
23. Lowry, O., and Rosebrough, N. (1951) *J. Biol. Chem. 193*, 265−275.
24. Thomas, P. E., Ryan, D., and Levin, W. (1976) *Anal. Biochem. 75*, 168−176.
25. Saribas, A. S., Valkova-Valchanova, M., Tokito, M. K., Zhang, Z., Berry, E. A., and Daldal, F. (1998) *Biochemistry 37*, 8105−8114.
26. Dutton, P. L. (1978) *Methods Enzymol. 54*, 411−435.
27. Gray, K., Dutton, P. L., and Daldal, F. (1994) *Biochemistry 33*, 723−733.
28. Ferrer, J. C., Guillemette, J. G., Bogumil, R., Inglis, S. C., Smith, M., and Mauk, A. G. (1993) *J. Am. Chem. Soc. 115*, 7507−7508.
29. Harbury, H. A., Cronin, J. R., Fanger, M. W., Hettinger, T. P., Murphy, A. J., Myer, Y. P., and Vinogradov, S. N. (1965) *Proc. Natl. Acad. Sci. U.S.A. 54*, 1658−1664.
30. Marchon, J. C., Mashiko, T., and Reed, C. A. (1982) in *Electron transport and oxygen utilisation* (Ho, C., Ed.) pp 67−72, Elsevier, Amsterdam, The Netherlands.
31. Ubbink, M., Campos, A. P., Teixeira, M., Hunt, N. I., Hill, H. A. O., and Canters, G. W. (1994) *Biochemistry 33*, 10051−10059.
32. Yeh, S.-R., and Rousseau, D. L. (1998) *Nat. Struct. Biol. 5*, 222−228.
33. Xu, Y., Mayne, L., and Englander, S. W. (1998) *Nat. Struct. Biol. 5*, 774−778.

BI990211K